# Requirement for Caspase-8 in NF-κB Activation by Antigen Receptor

Helen Su *et al.*

*Science* **307**, 1465 (2005);
DOI: 10.1126/science.1104765

organism and considerably less numerous than those in *B. fragilis*. This enhanced potential for variation and other genomic differences (SOM Text) may explain in part why *B. fragilis* is isolated more frequently from infection than *B. thetaiotaomicron*.

Surface polysaccharides are involved in establishing abscess formation (*10*). Ten separate gene clusters potentially involved in polysaccharide synthesis are evident in the genome sequence (table S3). The polysaccharide gene clusters A to H have genes similar to *wzx* and *wzy* that are involved in transfer of linked sugar repeats across the cytoplasmic membrane and repeat unit polymerization, respectively, but are lacking in genes associated with the export of polymer across the outer membrane. This suggests that these gene clusters are similar to the *Escherichia coli* group 4 O-antigen capsules (*11*) and is in keeping with the characteristic heterogeneity of the polysaccharide chain length after SDS–polyacrylamide gel electrophoresis (PAGE) and the EDL phenotype (*12*). A gene with some similarity to *E. coli wzz* (BF1708) that determines chain length is located within polysaccharide gene cluster J. Variation in the expression of BF1708 may explain the varying reports of presence (*13*) or absence (*14*) of repeating O-antigen units after PAGE.

Phase variation controlled by DNA inversion events has been reported in several other bacteria. For example, *Salmonella typhimurium* regulates the expression of a flagellar protein by using a single invertible promoter (*15*), and *E. coli* plasmids use shufflons to express one of several variant pilus proteins (*16*). Different species of *Mycoplasma* have been shown to regulate the expression of a number of surface proteins by using invertible promoters (*17*) or to use a shufflon system to express variable surface proteins (*8*). However, in each of these cases, the use of these mechanisms is restricted to a single system or class of surface molecules. As described here, *B. fragilis* uses DNA inversion to control a larger number or greater breadth of systems than in any other organism described to date, including surface proteins, polysaccharides, and regulatory systems. This may be related to its niche as a commensal and opportunistic pathogen, because the resulting diversity in surface structures could increase both immune invasion and the ability to colonize novel sites.

*Note added in proof*: The genome sequence of another strain of *B. fragilis* has recently been published (*19*), and the analysis is in general agreement with that presented here.


**References and Notes**

1. S. Patrick, in *Molecular Medical Microbiology*, M. Sussman, Ed. (Academic Press, London, 2002), pp. 1921–1948.
2. C. Erridge, A. Pridmore, A. Eley, J. Stewart, I. R. Poxton, *J. Med. Microbiol.* **53**, 735 (2004).
3. S. Patrick, J. H. Reid, A. Coffey, *J. Gen. Microbiol.* **132**, 1099 (1986).
4. S. Patrick, D. Gilpin, L. Stevenson, *Infect. Immun.* **67**, 4346 (1999).
5. S. Patrick *et al.*, *Microbiology* **149**, 915 (2003).
6. C. M. Krinos *et al.*, *Nature* **414**, 555 (2001).
7. M. J. Coyne, K. G. Weinacht, C. M. Krinos, L. E. Comstock, *Proc. Natl. Acad. Sci. U.S.A.* **100**, 10446 (2003).
8. I. Chambaud *et al.*, *Nucleic Acids Res.* **29**, 2145 (2001).
9. J. Xu *et al.*, *Science* **299**, 2074 (2003).
10. A. O. Tzianabos, A. B. Onderdonk, B. Rosner, R. L. Cisneros, D. L. Kasper, *Science* **262**, 416 (1993).
11. C. Whitfield, I. S. Roberts, *Mol. Microbiol.* **31**, 1307 (1999).
12. D. A. Lutton *et al.*, *J. Med. Microbiol.* **35**, 229 (1991).
13. I. R. Poxton, R. Brown, *J. Gen. Microbiol.* **132**, 2475 (1986).
14. A. A. Lindberg, A. Weintraub, U. Zahringer, E. T. Rietschel, *Rev. Infect. Dis.* **12** (suppl. 2), S133 (1990).
15. M. Silverman, J. Zieg, M. Hilmen, M. Simon, *Proc. Natl. Acad. Sci. U.S.A.* **76**, 391 (1979).
16. A. Gyohda, N. Furuya, A. Ishiwa, S. Zhu, T. Komano, *Adv. Biophys.* **38**, 183 (2004).
17. A. Horino, Y. Sasaki, T. Sasaki, T. Kenri, *J. Bacteriol.* **185**, 231 (2003).
18. The sequence and annotation of the genome have been submitted to the DNA Data Bank of Japan, European Molecular Biology Laboratory, and GenBank databases with accession numbers CR626927 (chromosome) and CR626928 (pBF9343) and are available with further details from www.sanger.ac.uk/Projects/B_fragilis/.
19. T. Kuwahara *et al.*, *Proc. Natl. Acad. Sci. U.S.A.* **101**, 14919 (2004).


20. We acknowledge the support of the Wellcome Trust Sanger Institute core sequencing and informatics groups. S.P. thanks M. Larkin (Queen's University Environmental Science and Technology Research Centre, Queen's University of Belfast) for the use of the laboratory and advice on DNA extraction methods. Supported by the Wellcome Trust through its Beowulf Genomics initiative.


**Supporting Online Material**

www.sciencemag.org/cgi/content/full/307/5714/1463/DC1
Materials and Methods
SOM Text
Figs. S1 and S2
Tables S1 to S4


16 August 2004; accepted 30 December 2004
10.1126/science.1107008


# Requirement for Caspase-8 in NF-κB Activation by Antigen Receptor


**Helen Su,[1]* Nicolas Bidère,[1]* Lixin Zheng,[1] Alan Cubre,[1] Keiko Sakai,[1] Janet Dale,[2] Leonardo Salmena,[3] Razqallah Hakem,[3] Stephen Straus,[2] Michael Lenardo[1]†**



**Caspase-8, a proapoptotic protease, has an essential role in lymphocyte activation and protective immunity. We show that caspase-8 deficiency (CED) in humans and mice specifically abolishes activation of the transcription factor nuclear factor κB (NF-κB) after stimulation through antigen receptors, Fc receptors, or Toll-like receptor 4 in T, B, and natural killer cells. Caspase-8 also causes the αβ complex of the inhibitor of NF-κB kinase (IKK) to associate with the upstream Bcl10-MALT1 (mucosa-associated lymphatic tissue) adapter complex. Recruitment of the IKKα,β complex, its activation, and the nuclear translocation of NF-κB require enzyme activity of full-length caspase-8. These findings thus explain the paradoxical association of defective apoptosis and combined immunodeficiency in human CED.**


The intracellular aspartate-specific cysteine protease caspase-8 initiates death receptor signaling for apoptosis (*1*). Recruitment into the death-signaling complex induces procaspase-8 oligomerization, followed by full processing into a highly active soluble tetramer (*2*, *3*). However, caspase-8 is also essential for lymphocyte activation and protective immunity in mice and humans (*4*, *5*). Patients with caspase-8 deficiency (CED) have defective apoptosis and immunodeficiency due to impaired activation of T, B, and natural killer (NK) lymphocytes (*4*).

Human peripheral blood leukocytes (PBLs) or mouse T cells treated with the pan-caspase inhibitor benzyloxycarbonylvalyl-alanyl–aspartic acid (*O*-methyl)–fluoro-methylketone (zVAD) have reduced antigen receptor–induced expression of interleukin-2 (IL-2) and its receptor subunit CD25 (*4*, *6*, *7*). Because nuclear factor κB (NF-κB) is required for IL-2 and CD25 gene transcription as well as lymphocyte activation (*8*, *9*), we examined this transcription factor in cells exposed to caspase inhibitor. NF-κB family members—Rel (c-*rel*), RelA (p65), RelB, NF-κB1 (p105/50), and NF-κB2 (p100/52)—regulate gene transcription as dimers (*8*, *9*).


[1]Laboratory of Immunology, National Institute of Allergy and Infectious Diseases, National Institutes of Health, Bethesda, MD 20892, USA. [2]Laboratory of Clinical Infectious Diseases, National Institute of Allergy and Infectious Diseases, National Institutes of Health, Bethesda, MD 20892, USA. [3]Ontario Cancer Institute, University of Toronto, Toronto, Ontario M5G 2C1, Canada.

*These authors contributed equally to this work.
†To whom correspondence should be addressed. E-mail: lenardo@nih.gov

Lymphocyte stimulation causes phosphorylation and degradation of inhibitor of κB (IκB) proteins, leading to NF-κB nuclear translocation and transcriptional activation. Nuclear translocation of p65 or p50, which constitute the NF-κB heterodimer, was detected 5 min after T cell receptor (TCR) stimulation in control PBLs but not in cells treated with zVAD (Fig. 1A and fig. S1, A to C) (*10*). The difference occurred despite CD28 costimulation, indicating a defect in TCR signaling (Fig. 1A). Consistent with the zVAD effect, the caspase-8-deficient Jurkat T cell line I9.2 exhibited almost no NF-κB nuclear translocation after TCR stimulation compared to that in parental A3 cells (fig. S1, D to G, and fig. S2A), with a corresponding decrease in NF-κB nuclear binding activity but no effect on the binding activity of the transcription factors OCT1 or TFIID (Fig. 1B). TCR stimulation of I9.2 cells failed to induce transcription from an NF-κB promoter–driven luciferase reporter construct (Fig. 1C). NF-κB was also defective in A3 or primary human CD4$^+$ cells in which caspase-8 was specifically knocked down using short hairpin RNAs (shRNAs) (fig. S3, A to C), A3 or mouse EL-4 T cells pretreated with zVAD (fig. S3, D to F, and fig. S4, A to D), and in caspase-8-deficient T cells from conditional knockout mice (fig. S4, E and F). These effects appeared to be selective for the TCR signaling pathway, because tumor necrosis factor–α (TNF-α)–induced NF-κB activation was not affected by zVAD or caspase-8 deficiency (Fig. 1 and figs. S1 to S4). Moreover, all other early activation events examined were essentially unaffected (fig. S5) (*10*). Together, these results suggest a selective role for caspase-8 in NF-κB activation.

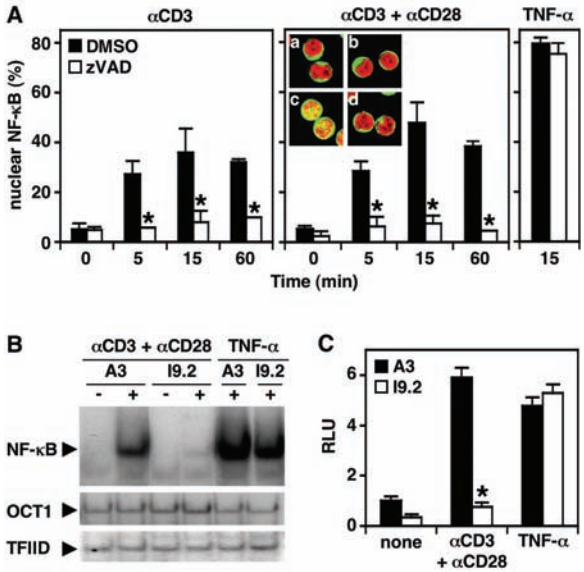


**Fig. 1.** Defective NF-κB translocation and transcriptional activation in CED T cells. (**A**) Quantitation of the fraction of cells by immunofluorescence confocal microscopy showing NF-κB p65 nuclear translocation. Results are shown as the mean ± SD for PBLs from three normal donors, with or without zVAD, and then stimulated with antibodies to CD3ε (anti-CD3ε) and anti-CD28 (1 μg/ml each), anti-CD3ε (1 μg/ml) alone, or TNF-α (10 ng/ml) as indicated. (Inset) Representative merged views of p65 (green), Hoechst (red), overlay (yellow) from unstimulated (a and b), or cells stimulated with anti-CD3ε and anti-CD28 (c and d), pretreated with dimethyl sulfoxide (DMSO) (a and c), or zVAD (b and d). (**B**) NF-κB gel shift of nuclear extracts prepared from A3 and I9.2 cells after 20 min of stimulation with anti-CD3ε and anti-CD28 (1 μg/ml each) (+), control (−), or TNF-α (10 ng/ml). OCT1 or TFIID gel shifts of the same nuclear extracts are shown. (**C**) Relative light units (RLU) of luciferase activity for an NF-κB luciferase reporter construct transfected into A3 or I9.2 cells and stimulated for 16 hours with anti-CD3ε, anti-CD28 (2 μg/ml each), and goat antibody to mouse immunoglobulin G (IgG) (5 μg per ml) or TNF-α (30 ng per ml) one day after transfection. Asterisk indicates $P < 0.05$ by the unpaired Student's *t* test for experimental compared to corresponding control.

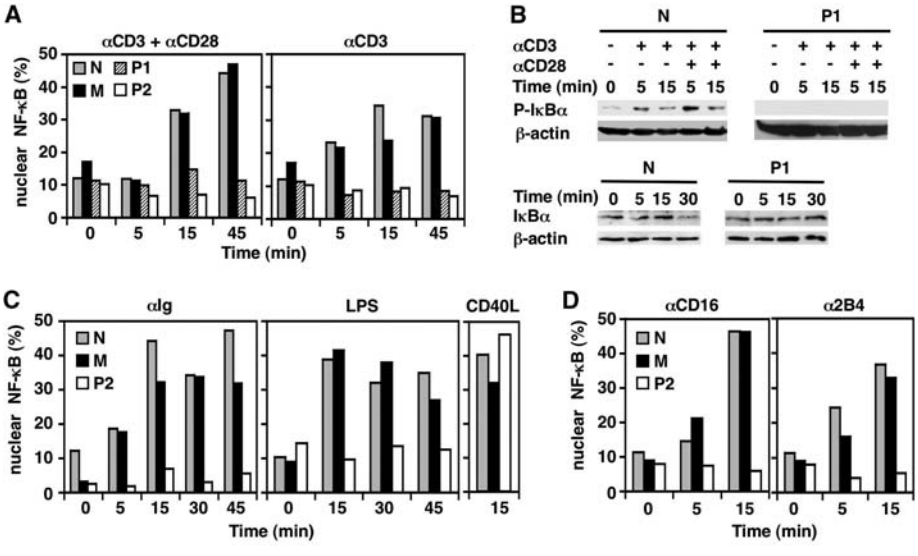


**Fig. 2.** Impaired NF-κB in lymphocytes from caspase-8-deficient humans. N, normal donor; M, healthy mother (+/*m*); P1, proband (*m*/*m*); P2, affected sibling (*m*/*m*). Genotype: +, normal; *m*, mutant. (**A**) Quantitation of the fraction of cells by immunofluorescence confocal microscopy showing NF-κB p65 nuclear translocation. T lymphocytes were stimulated with anti-CD3ε and anti-CD28 (1 μg/ml each) or anti-CD3ε (1 μg/ml) alone. (**B**) Lysates from stimulated T cells, immunoblotted for phosphorylated-IκBα (P-IκBα) and IκBα. (**C**) NF-κB p65 nuclear translocation in B cells stimulated with biotinylated anti-IgG (20 μg/ml) and streptavidin (20 μg/ml), lipopolysaccharide (LPS, 50 μg/ml), or CD40 ligand (CD40L, 2.5 μg/ml). (**D**) NF-κB p65 nuclear translocation in NK cells stimulated with anti-CD16 (20 μg/ml) or 2B4 (10 μg/ml) and goat antibody to mouse IgG (20 μg/ml).

We next examined NF-κB activation in PBLs from NIH CED family 66 (*4*). Early activation events in T cells were essentially normal, but NF-κB did not translocate to the nucleus after TCR stimulation in PBLs that were homozygous for CED (fig. S6, Fig. 2A, and fig. S7A). Notably, the heterozygous mother showed no such impairment, indicating that a single functional copy of the gene sufficed for NF-κB signaling.

Phosphorylation activates the IκB kinase (IKK) complex, composed of the two catalytic subunits IKKα and IKKβ and a regulatory subunit IKKγ (NEMO) (*8*, *9*). Active IKK phosphorylates IκBα, which marks IκBα for degradation, thereby liberating NF-κB for nuclear translocation and transcriptional activity. However, we saw no IκBα phosphorylation or degradation in TCR-stimulated PBLs from a CED patient (Fig. 2B and fig. S7I). Hence, caspase-8 was necessary for NF-κB activation after TCR stimulation.

We next evaluated NF-κB activation in B cells and NK cells. B cells from a CED patient failed to translocate NF-κB into the nucleus after B cell receptor (BCR) stimulation (Fig. 2C and fig. S7C). Ramos B cells, in which caspase-8 was knocked down using specific shRNAs, displayed a similar defect (fig. S7, F and G). NF-κB activation induced by lipopolysaccharide (LPS) requires signaling through Toll-like receptor 4 (TLR4). In B cells from a CED patient, but not an autoimmune lymphoproliferative syndrome patient bearing a Fas mutation (ALPS, Type Ia), NF-κB nuclear translocation was abrogated after LPS stimulation (Fig. 2C and fig. S7, C to E).

By contrast, NF-κB could be normally activated in CED B cells through CD40 (Fig. 2C and fig. S7C) (*11*). NK cells from CED patients failed to translocate NF-κB into the nucleus after FcγRIII or 2B4 (NK cell–activating receptor) stimulation (Fig. 2D and fig. S7H). NF-κB activation proceeds normally in caspase-8-deficient mouse embryo fibroblasts after TNF-α or Fas stimulation (*12*). Thus, CED impairs both adaptive immunoreceptor signaling and certain pathways of innate immunity that activate NF-κB.

Early TCR activation events link to NF-κB activation through protein kinase Cθ (PKCθ) activation (*13*, *14*). PKCθ phosphorylation recruits the CARMA1-Bcl10-MALT1 (CBM) complex to the immunological synapse (*15*, *16*). This complex of adapter molecules causes activation of the IKK complex. However, the CBM and IKK complexes do not appear to interact directly (*17*), and how the signal for NF-κB activation is conveyed between the two is not well understood (*15*, *16*, *18*). The amounts of active phosphorylated PKCθ were not altered by caspase-8 deficiency (fig. S5C). In normal Jurkat cells, IKKα phosphorylation occurred at 5 min after TCR stimulation, and IKKα,β and IκBα phosphorylation occurred maximally after 10 min, followed by IκBα degradation (Fig. 3A and fig. S8A). IKK phosphorylation coincided with the appearance of in vitro kinase activity using glutathione S-transferase (GST)–IκBα as a substrate (Fig. 3B). IKK phosphorylation, IκBα phosphorylation and degradation, and in vitro kinase activity were reduced in I9.2 cells (Fig. 3, A and B). Thus, caspase-8 acts between PKCθ and IKK in the NF-κB pathway.

We used coimmunoprecipitation and immunoblotting to show that TCR stimulation induced caspase-8 to associate with the Bcl10-MALT1 complex followed by recruitment of IKK (Fig. 3C). Formation of this complex coincided with IKK phosphorylation and activation at 10 min after stimulation. Absence of caspase-8 abrogated IKKα,β recruitment and activation by the CBM complex (Fig. 3, A and D). The adapter protein FADD associated with caspase-8 and Bcl10-MALT1 at an earlier time (5 min) but disappeared before the recruitment of IKK to form the holocomplex (Fig. 3E). Caspase-8 appears to act before IKK, because reconstituting I9.2 cells with constitutively active IKK restored NF-κB activation (fig. S8, B and C). Thus, caspase-8 is integral to the assembly and activation of the CBM-IKK complex in response to antigen receptors.

Our observation that zVAD blocks NF-κB activation after TCR stimulation suggests that caspase-8 enzymatic activity may be essential. Indeed, we found that wild-type caspase-8, but not the catalytically inactive C360S mutant (where $Cys^{360}$ is replaced by Ser), enhanced NF-κB responses to TCR stimulation in transfected I9.2 cells (Fig. 3F). We next tested caspase-8 autoprocessing mutants (D210A, D374A, and D384A) by substituting alanines for aspartic acid residues (*10*). These mutants increased NF-κB activity in I9.2 cells after TCR stimulation, indicating that enzymatic activity, but not autoprocessing, was required (Fig. 3F and fig. S8F). Consistent with this conclusion, only full-length forms of caspase-8, which are known to be enzymatically active (*2*, *3*), were detected in the CBM complex (Fig. 3E). We therefore used a more sensitive probe, biotinylated-VAD (b-VAD), which bonds covalently to the catalytic cysteine of active caspases. Precipitation of b-VAD detected a small amount of enzymatically active full-length caspase-8 in lysates from unstimulated T cells (Fig. 3G). TCR stimulation caused activation of full-length caspase-8 and induced physical interaction with Bcl10 at times when IKK was recruited, phosphorylated, and active (Fig. 3G). Depletion of the b-VAD–bound species revealed that only a minor fraction (10 to 15%) of the total

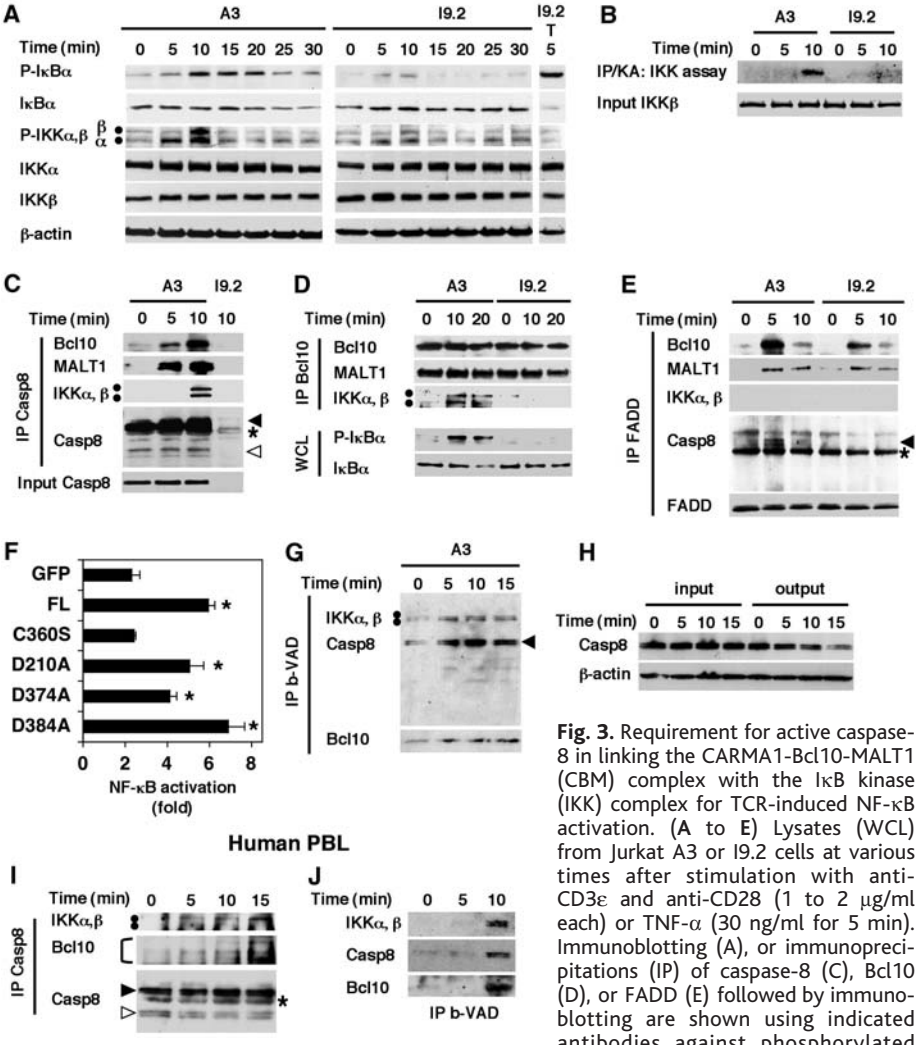


**Fig. 3.** Requirement for active caspase-8 in linking the CARMA1-Bcl10-MALT1 (CBM) complex with the IκB kinase (IKK) complex for TCR-induced NF-κB activation. (**A** to **E**) Lysates (WCL) from Jurkat A3 or I9.2 cells at various times after stimulation with anti-CD3ε and anti-CD28 (1 to 2 μg/ml each) or TNF-α (30 ng/ml for 5 min). Immunoblotting (A), or immunoprecipitations (IP) of caspase-8 (C), Bcl10 (D), or FADD (E) followed by immunoblotting are shown using indicated antibodies against phosphorylated IκBα (P-IκBα), IκBα, the α and/or β subunits of phosphorylated IKK (P-IKK), Bcl10, MALT1, caspase-8, or FADD. Solid arrowhead indicates full length (p54 and 52). Open arrowhead indicates partly processed (p43 and 41) forms of caspase-8. Asterisks indicate Ig heavy chain in immunoprecipitates. For (B), IKK in vitro kinase activity was assessed in coimmunoprecipitates of IKKγ by the ability to phosphorylate GST-IκBα. (**F**) Activity of an NF-κB luciferase reporter in I9.2 cells transfected with the indicated caspase-8 expression constructs. GFP, green fluorescence protein–expressing vector; FL, full-length wild-type caspase-8. Cells were stimulated for 24 hours with anti-CD3ε and anti-CD28 (2 μg/ml each) and goat antibody to mouse IgG (5 μg/ml) 2 days after transfection. Asterisks indicate $P < 0.001$ by the Student's $t$ test compared to the GFP control. (**G**) Biotinylated-VAD (b-VAD) was incubated with protein lysates after TCR stimulation as in (F), then precipitated with streptavidin, and IKK, caspase-8, and Bcl10 proteins were detected by immunoblotting. (**H**) Lysates before (input) and after (output) precipitation of b-VAD–bound proteins, shown immunoblotted for full-length caspase-8 and β-actin. (**I** and **J**) Lysates from human PBLs were prepared at various times after stimulation with anti-CD3ε and anti-CD28 (1 μg/ml each). IP of caspase-8 (I) or using b-VAD (J) were followed by immunoblotting to detect IKKα,β, Bcl10, and caspase-8 proteins.

caspase-8 became enzymatically active after TCR stimulation (Fig. 3H and fig. S8G). Hence, NF-κB activation by antigen receptors requires enzyme activity of full-length caspase-8. In the NF-κB–activating holocomplex, caspase-8 appears to be bound, unprocessed, and only weakly activated, by contrast to caspase-8 in a death-inducing complex (*2*, *3*).

Caspase-8 now emerges both as a pivotal molecule for death-receptor signaling and as a selective signal transducer for NF-κB during the early genetic response to an antigen. This explains the requirement for caspase activity and caspase-8 for lymphocyte activation and c-*rel* responses after antigen receptor stimuli (*4*–*7*, *19*). Full-length, unprocessed, but active caspase-8 serves as a crucial link for the CBM and IKK complexes leading to NF-κB activation not only in lymphoid cell lines, but also in freshly isolated human lymphocytes (Fig. 3, I and J). After antigen receptor stimulation, MALT1-dependent recruitment of the ubiquitin ligase TRAF6 to the CBM complex may enhance regulatory polyubiquitination of IKKγ (*20*, *21*). IKKγ ubiquitination, but not phosphorylation of IKKα,β, occurred in the absence of caspase-8, indicating that ubiquitination may be necessary but not sufficient for IKK activation (fig. S8H).

CED patients manifest certain diagnostic criteria for ALPS, most notably impaired lymphocyte apoptosis (*22*). However, the combined T, B, and NK cell immunodeficiency is not seen in ALPS patients with Fas, Fas ligand, or caspase-10 mutations. Our findings reveal how a single protease regulates both lymphocyte proliferation and programmed death through different molecular forms. The molecular mechanism we have unveiled may be useful in understanding and treating other varieties of immunodeficiency and disordered lymphocyte homeostasis.

### References and Notes


1. A. Ashkenazi, V. M. Dixit, *Science* **281**, 1305 (1998).
2. K. M. Boatright *et al.*, *Mol. Cell. Biol.* **11**, 529 (2003).
3. M. Donepudi, A. Mac Sweeney, C. Briand, M. G. Grutter, *Mol. Cell. Biol.* **11**, 543 (2003).
4. H. J. Chun *et al.*, *Nature* **419**, 395 (2002).
5. L. Salmena *et al.*, *Genes Dev.* **17**, 883 (2003).
6. N. J. Kennedy, T. Kataoka, J. Tschopp, R. C. Budd, *J. Exp. Med.* **190**, 1891 (1999).
7. A. Alam, L. Y. Cohen, S. Aouad, R. P. Sekaly, *J. Exp. Med.* **190**, 1879 (1999).
8. S. Ghosh, M. Karin, *Cell* **109**, S81 (2002).
9. Q. Li, I. M. Verma, *Nat. Rev. Immunol.* **2**, 725 (2002).
10. Materials and methods are available as supporting material on *Science* Online.
11. B. Zarnegar *et al.*, *Proc. Natl. Acad. Sci. U.S.A.* **101**, 8108 (2004).
12. E. E. Varfolomeev *et al.*, *Immunity* **9**, 267 (1998).
13. Z. Sun *et al.*, *Nature* **404**, 402 (2000).
14. X. Lin, A. O'Mahony, Y. Mu, R. Geleziunas, W. C. Greene, *Mol. Cell. Biol.* **20**, 2933 (2000).
15. M. Thome, *Nat. Rev. Immunol.* **4**, 348 (2004).
16. P. C. Lucas, L. M. McAllister-Lucas, G. Nunez, *J. Cell Sci.* **117**, 31 (2004).
17. P. C. Lucas *et al.*, *J. Biol. Chem.* **276**, 19012 (2001).
18. L. Yu, M. J. Lenardo, *Science* **302**, 1515 (2003).
19. M. Falk *et al.*, *J. Immunol.* **173**, 5077 (2004).
20. L. Sun, L. Deng, C. K. Ea, Z. P. Xia, Z. J. Chen, *Mol. Cell. Biol.* **14**, 289 (2004).
21. H. Zhou *et al.*, *Nature* **427**, 167 (2004).
22. M. C. Sneller *et al.*, *Blood* **89**, 1341 (1997).

23. Molecular interaction data have been deposited in the Bimolecular Interaction Network Database (BIND) with accession codes 196525, 196526, 196446, and 196449. We thank I. Stefanova for tyrosine phosphorylation experiments; V. Barr and L. Samelson for T cell spreading experiments; E. Lee and G. Wang for technical assistance; J. Blenis, R. Siegel, L. Van Parijs, V. Horejsi, A. Jain, V. Dixit, M. Peter, and Z. Liu for materials and reagents; D. Stephany, K. Holmes, and O. Schwartz for flow cytometry and microscopy assistance; F. Dugan and J. Davis for clinical assistance; L. Sun, Z. Chen, Z. Liu, and S. Feske for advice on IKK kinase assay and calcium flux; L. Yu and R. Siegel for helpful discussions; and R. Germain, L. Samelson, and J. Puck for critically reading the manuscript. H.S. is a fellow of the Cancer Research Institute. N.B. is supported by an Association pour la Recherche contre le Cancer (ARC) fellowship.

**Supporting Online Material**

www.sciencemag.org/cgi/content/full/307/5714/1465/DC1
Materials and Methods
SOM Text
Figs. S1 to S8
References

1 September 2004; accepted 4 January 2005
10.1126/science.1104765

# Impaired Thermosensation in Mice Lacking TRPV3, a Heat and Camphor Sensor in the Skin

**Aziz Moqrich,[1,2]* Sun Wook Hwang,[1]* Taryn J. Earley,[1] Matt J. Petrus,[2] Amber N. Murray,[1] Kathryn S. R. Spencer,[1] Mary Andahazy,[2] Gina M. Story,[1] Ardem Patapoutian[1,2]†**

**Environmental temperature is thought to be directly sensed by neurons through their projections in the skin. A subset of the mammalian transient receptor potential (TRP) family of ion channels has been implicated in this process. These "thermoTRPs" are activated at distinct temperature thresholds and are typically expressed in sensory neurons. TRPV3 is activated by heat (>33°C) and, unlike most thermoTRPs, is expressed in mouse keratinocytes. We found that TRPV3 null mice have strong deficits in responses to innocuous and noxious heat but not in other sensory modalities; hence, TRPV3 has a specific role in thermosensation. The natural compound camphor, which modulates sensations of warmth in humans, proved to be a specific activator of TRPV3. Camphor activated cultured primary keratinocytes but not sensory neurons, and this activity was abolished in TRPV3 null mice. Therefore, heat-activated receptors in keratinocytes are important for mammalian thermosensation.**

Thermosensation is thought to be directly mediated by sensory neurons of the dorsal root ganglia (DRGs) that terminate as free nerve endings within the dermal and epidermal layers of the skin (*1*). Six members of the TRP family of ion channels are activated by distinct thresholds of temperature (*2*). The expression of most of these thermoTRPs in DRG neurons is consistent with a role in thermosensation. TRPV3 is activated by warm temperatures above 33°C and exhibits increased response at noxious higher temperatures (*3*–*5*). Mouse TRPV3 is distinct among thermoTRPs because it is expressed in keratinocytes but not in DRGs (*3*). TRPV4, a related innocuous heat-activated ion channel, is expressed in both DRGs and skin (*6*–*8*). The prevailing model that temperature is sensed directly by DRG neurons calls into question whether keratinocyte-derived TRPV3 is involved in thermosensation.

To specifically determine the in vivo function of TRPV3, we used a knockout construct to target the mouse gene encoding TRPV3 by deleting exons encoding the putative pore region and adjacent transmembrane segments five and six, essential domains of the ion channel (fig. S1A). Mice carrying two alleles of the TRPV3 mutation survived through adulthood at the expected Mendelian ratio (fig. S1B). The reverse transcription polymerase chain reaction (RT-PCR) was used to evaluate the expression of TRPV3 in the mutant mice. We used two sets of primers to evaluate TRPV3 transcripts, one pair spanning the deleted region and another preceding it (fig. S1, A and C) (*9*). TRPV3 transcript from the skin of homozygous knockout mice was not detected with the first pair of primers and was detected at low levels with the second pair (fig. S1C). In contrast,

[1]Department of Cell Biology, Scripps Research Institute, La Jolla, CA 92037, USA. [2]Genomics Institute, Novartis Research Foundation, San Diego, CA 92121, USA.

*These authors contributed equally to this work.
†To whom correspondence should be addressed. E-mail: ardem@scripps.edu